

## Effect of the nematic range on the critical behavior and anisotropy of the heat transport parameters at the smectic-*A*–nematic phase transition

F. Mercuri,\* U. Zammit, and M. Marinelli

*Dipartimento di Ingegneria Meccanica, Università di Roma and Sezione INFM "Tor Vergata," Via O. Raimondo 1, 00173 Roma, Italy*

(Received 9 June 1997)

The photopyroelectric technique has been used to study the specific heat, the thermal conductivity, and the thermal diffusivity at the smectic-*A*–nematic phase transition of homeotropic and planar samples of 4-*n*-pentylphenylthiol-4'-*n*-octyloxythiolbenzoate (8S5) and 4-*n*-nonyl-4'-cyanobiphenyl (9CB). It has been shown that, as in the case of 4-*n*-octyl-4'-cyanobiphenyl (8CB), the thermal conductivity remains approximately constant at the smectic-*A*–nematic (*A*-*N*) phase transition and therefore the specific heat and the thermal diffusivity have the same critical exponent. Though the *A*-*N* transition in 9CB is quite close to the tricritical point, it turns out that tricriticality does not affect the critical behavior of the thermal conductivity. The temperature dependence of the thermal conductivity anisotropy, which can be considered as a macroscopic order parameter, has been reported for all the samples investigated. It has been shown that the influence of smectic ordering on the order parameter becomes progressively more important when the *A*-*N* tricritical point is approached. [S1063-651X(98)02201-6]

PACS number(s): 64.70.Md

### INTRODUCTION

Photothermal techniques have been applied recently to the study of the critical behavior of dynamic thermal parameters, such as the thermal conductivity ( $k$ ) and the thermal diffusivity ( $D = k/\rho c$ , where  $\rho$  is the density and  $c$  is the specific heat), close to liquid-crystal phase transitions [1]. These techniques need to introduce a small temperature gradient in the sample to obtain a good signal-to-noise ratio, thus allowing a high-temperature resolution in the determination of the thermal parameters close to the phase transition. The results available in the literature, however, do not provide a clear picture of the critical behavior of  $D$  and  $k$  and the lack of any quantitative theoretical prediction makes their interpretation extremely difficult. It is worthwhile to note that these difficulties in understanding the critical behavior of the thermal transport parameters are not surprising at all if one considers that even the physical mechanism of heat transport in liquid crystals, away from the transition temperature, has not been explained on a quantitative basis.

A divergence in the thermal conductivity and a dip in the thermal diffusivity have been reported at the smectic-*A*–hexatic-*B* transition of *n*-hexyl-4'-*n*-pentyloxybiphenyl-4-carboxylate (65OBC) [2]. Again a divergence in  $k$  has been found at the smectic-*A*–smectic-*C* (*A*-*C*) transition of *N*-(4-*n*-heptyloxybenzylidene)-4'-*n*-butylaniline (7O.4), while a dip with a superimposed peak at the transition temperature has been found in  $D$  [3]. A similar behavior has been reported for the *A*-*C* transition of racemic 4-(3-methyl-2-chlorobutanoyloxy)-4'-heptyloxybiphenyl (A7) [4], the peak in  $D$  at  $T_c$  being much more pronounced than the one of 7O.4. Such behavior was related by the authors to the fact that the latter compound is much closer to the mean-field tricritical point than 7O.4. Measurements are

also available at the smectic-*A*–nematic (*A*-*N*) transition for 4-*n*-pentylphenylthiol-4'-*n*-octyloxybenzoate (8S5) [1] and 4-*n*-octyl-4'-cyanobiphenyl (8CB) [5], compounds having different nematic ranges. In both cases, a dip in the diffusivity and a smooth conductivity have been found close to the transition temperature. In the case of 8CB, measurements were performed on aligned samples, but no differences were found between the homeotropic and planar cases.

Though the results are puzzling, the situation is somewhat less complicated with respect to what has been found in the case of magnetic materials where the same transition in different materials showed different behavior for the thermal conductivity [6]. On the contrary, in the case of liquid crystals so far, compounds having the same transition have shown the same  $k$  behavior. Collective long-range phenomena and in particular nondissipative mode couplings could be responsible for the divergence of  $k$  for the *A*-*C* transition [4,7], while the smooth  $k$  behavior obtained for the *A*-*N* transition could be explained either with a dissipative mode coupling between the nonconserved order-parameter mode and the conserved energy density [7] or, more simply, assuming that the heat conduction is governed by short-range processes. The influence of tricriticality on the  $k$  and  $D$  critical behavior is another open question: While it seems strongly relevant in the case of the *A*-*C* transition [4], the situation is not clear for the *A*-*N* one. For 8S5 [1] and 8CB [5], the conductivity close to  $T_{AN}$  could be fit with a linear temperature dependence and it was therefore possible to describe the  $c$  and  $D$  critical behavior with the same critical exponent. A very small increase in  $k$  at the transition temperature was, however, detected in the latter case. It should be noted that 8CB is much closer to the tricritical point than 8S5, but not close enough to show a tricritical behavior.

The aim of this paper is to try to clarify the role of tricriticality on the heat transport parameters, in the case of the *A*-*N* transition, in compounds with different nematic ranges. The photopyroelectric technique has been used to determine

\*Electronic address: mercuri@utovrm.it

simultaneously the specific heat, the thermal conductivity, and the thermal diffusivity on aligned samples of 8S5 and 4-*n*-nonyl-4'-cyanobiphenyl (9CB) with a MacMillan ratio  $T_{AN}/T_{NI}$  of 0.936 and 0.994, respectively. The results have been compared with the ones already reported for 8CB [5], which has a  $T_{AN}/T_{NI}=0.977$ . It turns out that, in the critical region,  $k$  behaves in a similar smooth fashion in all the investigated samples, thus showing no influence of tricriticality. On the other hand, the width of the nematic range affects the thermal conductivity anisotropy. In fact, below  $T_{AN}$ ,  $k_{\parallel} - k_{\perp}$  (where  $\parallel$  and  $\perp$  refer to homeotropic and planar alignments, respectively) shows a feature that becomes more evident as the tricritical point is approached. This feature results from the contribution of the smectic ordering to the orientational order parameter. An analysis of the results in terms of a simple qualitative picture for the heat conduction mechanism previously proposed [8] will be given.

### EXPERIMENT

A photopyroelectric setup [9] has been used to determine simultaneously  $c$ ,  $k$ , and  $D$ , the sample density  $\rho$  being known. In the configuration we have used, the sample is sandwiched between a glass plate and a pyroelectric transducer. One of the sample surfaces was periodically heated and the temperature oscillation introduced at the opposite surface, which is estimated to be less than 1 mK, was detected by the transducer. The amplitude and the phase of the photopyroelectric signal, which depends on the sample thermal parameters [9], were analyzed by a lock-in amplifier. The transducer was a 300  $\mu\text{m}$  thick LiTaO<sub>3</sub> single crystal and the sample was 30  $\mu\text{m}$  thick. The surface of the glass plate in contact with the liquid crystal was coated with a 200-nm optically opaque Ti layer, which was thermally thin and therefore had a negligible effect in the heat diffusion process. A 5 mW He-Ne laser, acousto-optically modulated at 64 Hz and absorbed by the metallic coating, was the heating source. The sample and the transducer were contained in an oven. The intensity of the heating beam and sample heating rate were decreased as much as possible to minimize the effect of thermal gradients. It is well known that the thermal gradients, together with the sample purity, are responsible for the "rounding" that affects data points very close to the transition temperature. The width of the rounding region, which in the case of 8CB was about 5 mK from  $T_{AN}$  on either side of the transition, can be used to derive an upper limit for the extent to which thermal gradients in the sample affect the resolution of the measurements. For a temperature scan on a wide temperature range, the heating rate was about 20 mK/min, while for high-resolution measurements close to a phase transition, the rate was 0.5 mK/min. No substantial differences were found in the determination of the thermal parameters when taking into account the temperature dependence of the sample density [10], which in the case of 9CB shows a variation of about 2% in the temperature range 30 °C–60 °C, or when considering it as a constant. Samples have been recrystallized several times before their use.

A polarizing microscope was used to check the alignment. Homeotropic alignment was achieved by treating the glass plate and the pyroelectric surfaces in contact with the liquid crystal with a surfactant agent consisting of a solution of

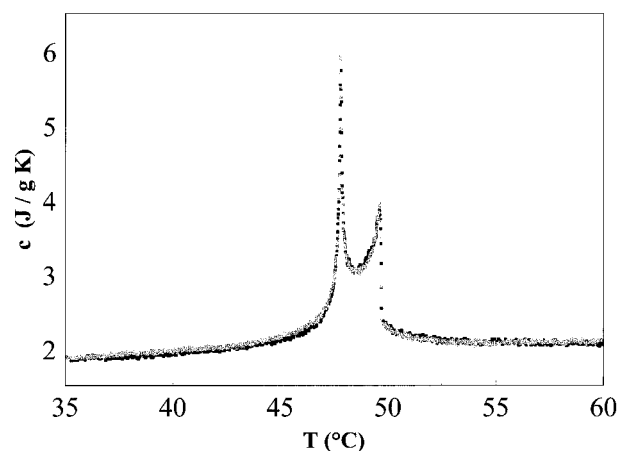


FIG. 1. Specific heat as a function of temperature for homeotropic (light gray dots) and planar (dark dots) 9CB samples.

trimethylcetylammmonium bromide. In order to achieve optimum alignment, the volume fraction of the solution was varied and the  $k_{\parallel}$  value at a fixed temperature was monitored. We observed a maximum of this value at the concentration value of the surfactant of about 5% in weight. Bearing in mind that, as shown later on in more detail, improvements in the alignment result in an increase of  $k_{\parallel}$  and in a decrease of  $k_{\perp}$ , we used such a value of the surfactant concentration for optimum homeotropic alignment. Planar alignment was obtained by sputtering a thin quartz film at a grazing angle on both the surfaces in contact with the liquid crystal and a procedure similar to the one mentioned above was used to optimize the deposition conditions

### RESULTS

Figure 1 shows the specific heat for two 9CB liquid-crystal samples with homeotropic and planar alignments in the temperature range 35 °C–60 °C. As expected, the two curves superimpose quite well in the whole temperature range investigated. The same data sets for the signal amplitude and phase from which  $c$  values have been calculated

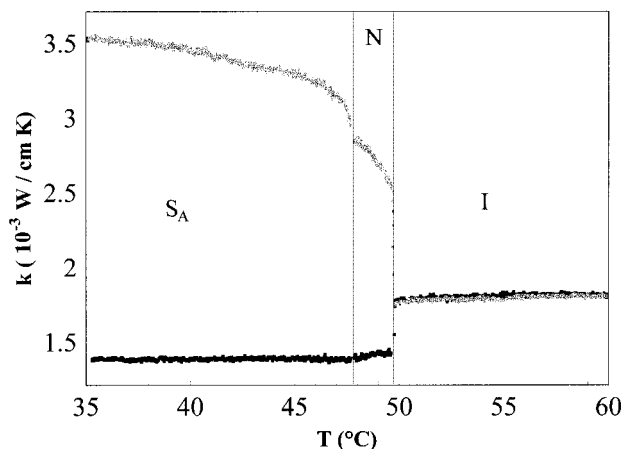


FIG. 2. Thermal conductivity as a function of temperature for homeotropic (light gray dots) and planar (dark dots) 9CB samples.

TABLE I. Values of the adjustable fitting parameters for the specific heat  $c$ , the thermal conductivity  $k$ , and the thermal diffusivity  $D$  for (a) homeotropic and (b) planar 9CB samples.

Fit	Parameter	$\alpha$	$A^+/A^-$	$T_c$ (K)	$B$ (J/g K)	$E$ (J/g K)	$A^-$ (J/g K)	$D^-$	$D^+$	$H$ (W/cm K)	$G$ (W/cm K <sup>2</sup> )	$\chi^2$
1a	$c$	$0.52 \pm 0.03$	$0.9 \pm 0.2$	$321.003 \pm 0.007$	$2.9 \pm 0.3$	$0.4 \pm 0.3$	$0.6 \pm 0.1$	$-2 \pm 1$	$-1.7 \pm 0.9$			1.08
2a	$D_{\parallel}$	$0.52 \pm 0.04$	$0.94 \pm 0.09$	$321.005 \pm 0.005$	$2.8 \pm 0.2$	$0.2 \pm 0.4$	$0.66 \pm 0.09$	$-1.9 \pm 0.7$	$-1.9 \pm 0.9$	$(2.7 \pm 0.2) \times 10^{-3}$	$(-1 \pm 2) \times 10^{-3}$	0.98
3a	$k_{\parallel}$									$(2.7 \pm 0.1) \times 10^{-3}$	$(-1 \pm 2) \times 10^{-4}$	1.11
1b	$c$	$0.52 \pm 0.04$	$0.98 \pm 0.09$	$321.002 \pm 0.005$	$2.9 \pm 0.2$	$0.5 \pm 0.3$	$0.5 \pm 0.1$	$-1.9 \pm 0.9$	$-1.9 \pm 0.9$			1.00
2b	$D_{\perp}$	$0.52 \pm 0.03$	$0.9 \pm 0.2$	$321.000 \pm 0.005$	$2.9 \pm 0.2$	$0.2 \pm 0.4$	$0.57 \pm 0.08$	$-2.0 \pm 0.5$	$-1.9 \pm 0.6$	$(1.29 \pm 0.06) \times 10^{-3}$	$(0 \pm 5) \times 10^{-4}$	1.01
3b	$k_{\perp}$									$(1.29 \pm 0.03) \times 10^{-3}$	$(1 \pm 2) \times 10^{-4}$	1.01

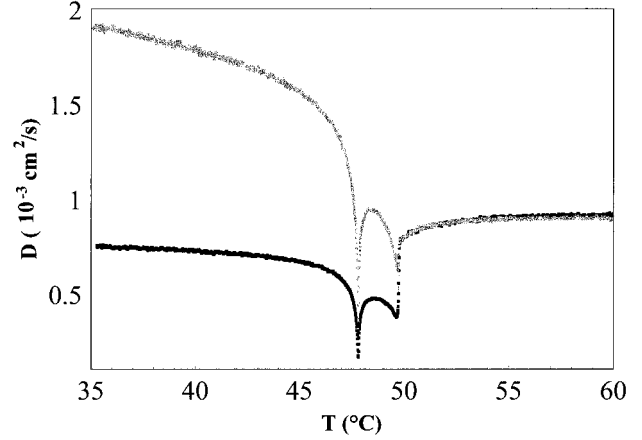


FIG. 3. Thermal diffusivity as a function of temperature for homeotropic (light gray dots) and planar (dark dots) 9CB samples.

have been also used to obtain the thermal conductivity and the thermal diffusivity.

Figure 2 shows the temperature dependence of  $k_{\parallel}$  and  $k_{\perp}$  in 9CB. In the isotropic phase the two data sets coincide and the values remain fairly constant from the  $N-I$  transition temperature up to 60 °C. A discontinuity is clearly evident at  $T_{NI}$  in both cases, with an increase of  $k_{\parallel}$  that is larger than the corresponding decrease of  $k_{\perp}$ . In the nematic phase  $k_{\parallel}$  increases with decreasing temperature, but the rate of such an increase shows a drastic change just below the  $A-N$  transition temperature. Finally, well within the smectic phase,  $k_{\parallel}$  seems to tend to a saturation value. On the other hand, a slight decrease of  $k_{\perp}$  with decreasing temperature has been obtained in the nematic phase, while its value remains fairly constant in the smectic phase down to 35 °C.

Figure 3 shows  $D_{\parallel}$  and  $D_{\perp}$  temperature scans in 9CB. Again, the two superimpose in the disordered phase and show a dip at the  $N-I$  and  $A-N$  transition temperature. The values of  $D_{\parallel}$  are always larger than the value of  $D_{\perp}$  in the nematic and in the smectic phases and this is of course due to the thermal conductivity anisotropy. The temperature dependence of  $D_{\perp}$  in the smectic phase, however, is essentially connected to the specific-heat behavior since  $k_{\perp}$  is approximately flat in that temperature region. The same happens over the transition temperature, where the dips in  $D$  seem to originate from the peaks in the specific heat.

To check in more detail this conclusion, high-resolution measurements have been performed close to the  $A-N$  transition temperature. Figure 4 show the specific-heat behavior vs the reduced temperature for homeotropic [Fig. 4(a)] and planar [Fig. 4(b)] samples, with the solid line representing the best-fit curve and the dotted one corresponding to data points in the rounding region that have not been considered in the fit. The data for the specific heat have been fit to the expression

$$c = B + E(T - T_c) + A^{\pm} |T - T_c|^{-\alpha} (1 + D^{\pm} |T - T_c|^{0.5}),$$

where the plus and minus signs refer to  $T > T_c$  and  $T < T_c$ , respectively and where we consider  $(T - T_c)$  as  $(T - T_c)/[1 \text{ (K)}]$ . The results of the fit have been reported in Table I. The two fits for homeotropic and planar samples, as ex-

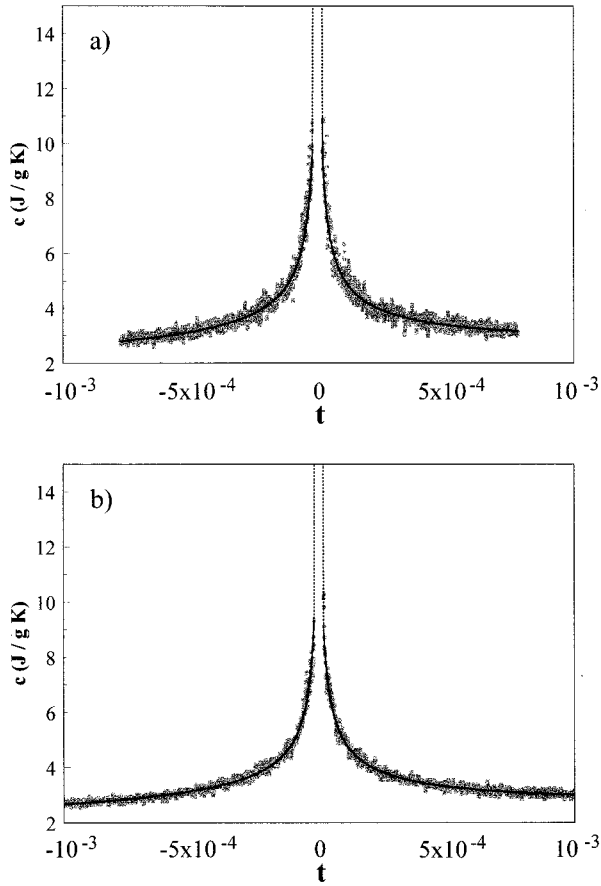


FIG. 4. High-resolution measurements of the specific heat as a function of the reduced temperature  $t = (T - T_{AN})/T_{AN}$  for (a) homeotropic and (b) planar 9CB samples. The solid line represents the best-fit curve. The dotted line corresponds to a temperature region that has not been considered in the fit.

pected, are quite similar, showing a critical exponent close to the tricritical one  $\alpha=0.5$  and in a good agreement with previously reported results [11]. The difference between the two amplitude ratios is within the statistical uncertainty, while, as expected [12], the ratio between the parameters  $D$  in the fit is

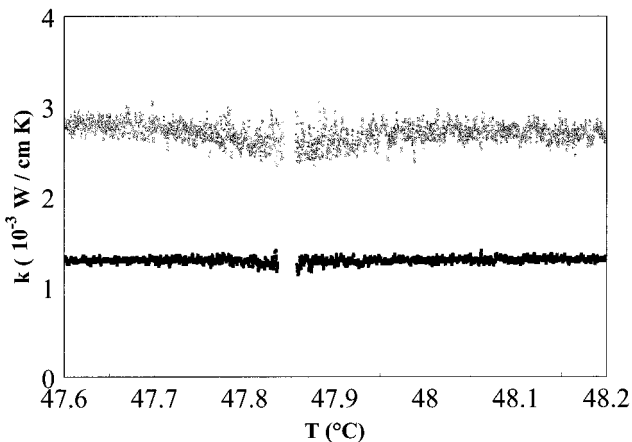


FIG. 5. High-resolution measurements of the thermal conductivity as a function of temperature close to  $T_{AN}$  for homeotropic (light gray dots) and planar (dark dots) 9CB samples.

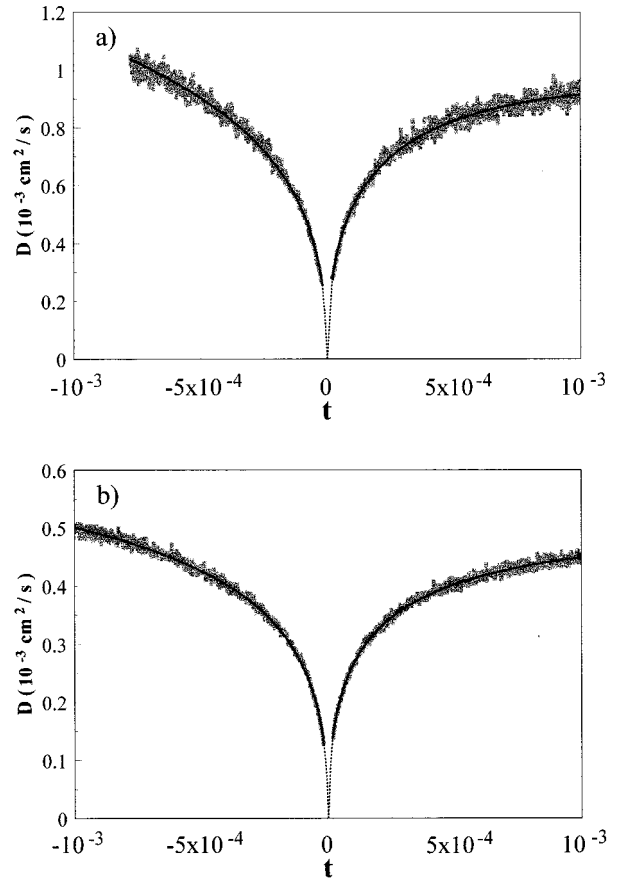


FIG. 6. High-resolution measurements of the thermal diffusivity as a function of the reduced temperature  $t = (T - T_{AN})/T_{AN}$  for (a) homeotropic and (b) planar 9CB samples. The solid line represents the best-fit curve. The dotted line corresponds to a temperature region that has not been considered in the fit.

approximately 1 in both cases. It should be noted that the tricritical value of  $A^+/A^-$  is not universal in the experimentally accessible temperature range [13], but a value of approximately 1 has been obtained for polar cyanobiphenyls [14].

Figure 5 shows the temperature dependence of  $k_{\parallel}$  and  $k_{\perp}$  in 9CB in the critical region. In both cases the thermal conductivity remains smooth over the whole temperature region investigated. A sharp and narrow peak close to the transition temperature was obtained in photoacoustic measurements of the  $k$  critical behavior in a nonaligned 9CB sample [15]. It has been shown that the photoacoustic technique needs to introduce in the sample a larger thermal gradient than the one needed by the photopyroelectric technique [16] and our conclusion is therefore that the very narrow peak shown in those data is at least partially contained in the rounding region due to thermal gradients. Figures 6(a) and 6(b) show  $D_{\parallel}$  and  $D_{\perp}$  vs reduced temperature and the data have been fitted with the expression

$$D = \frac{H + G(T - T_c)}{B + E(T - T_c) + A^{\pm} |T - T_c|^{-a} (1 + D^{\pm} |T - T_c|^{0.5})};$$

the fit results are reported in Table I. It is evident that it is

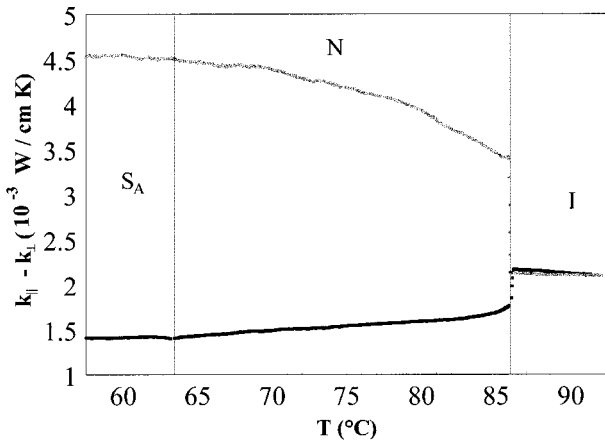


FIG. 7. Thermal conductivity as a function of temperature for homeotropic (light gray dots) and planar (dark dots) 8S5 samples.

possible to fit  $k$  with a linear temperature dependence and that the anomaly in the diffusivity depends on the specific-heat anomaly.

Figure 7 shows the temperature dependence of  $k_{\parallel}$  and  $k_{\perp}$  of 8S5. Some differences with respect to 9CB should be noted. No features appear in both  $k_{\parallel}$  and  $k_{\perp}$  close to  $T_{AN}$ , which remains quite smooth over the entire transition region and seems to have reached a saturation value in the smectic phase. Moreover, the decrease of  $k_{\perp}$  in the nematic phase with decreasing temperature is more evident than in 9CB. On the other hand, as in the case of 9CB,  $k_{\perp}$  remains approximately constant in the smectic phase.

Figure 8 shows the temperature dependence of the anisotropy in the thermal conductivity  $k_{\parallel} - k_{\perp}$  of 8S5, 8CB, and 9CB. It is well known that a macroscopic order parameter can be defined by extracting the anisotropic part of a quantity that has a tensorial nature in the ordered phases [17]. Thermal conductivity fulfills such conditions and we can therefore define  $k_{\parallel} - k_{\perp}$  as a macroscopic order parameter. Though the macroscopic and microscopic order parameters are related, a proportionality between the two can be quantitatively derived only in the case of magnetic susceptibility

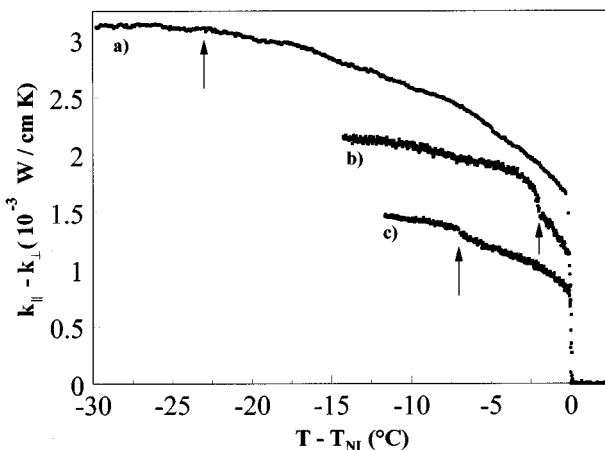


FIG. 8. Thermal conductivity anisotropy as a function of  $T - T_{NI}$  for (a) 8S5 (b) 9CB, and (c) 8CB. The arrows indicate the A-N transition temperature for the three compounds.

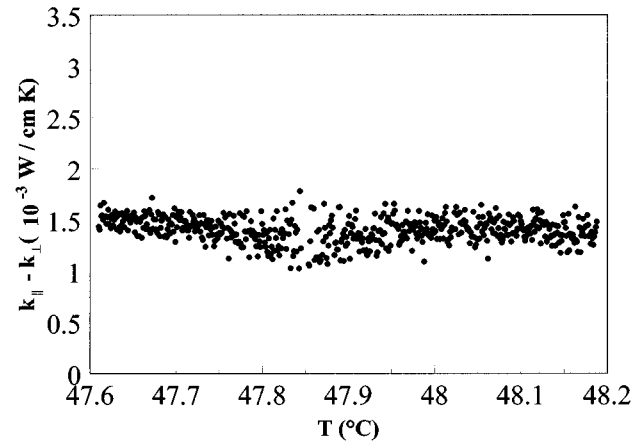


FIG. 9. High-resolution measurements of the thermal conductivity anisotropy as a function of temperature close to  $T_{AN}$  for 9CB.

[17]. In many other cases, the two quantities have been considered to be proportional, but this is based on an arbitrary assumption about the correlation function [17].

The behavior of the order parameter at the transition temperature depends on the order of the phase transition: A discontinuity is expected for a first-order transition, while the order parameter remains continuous for a second-order one. In the isotropic phase,  $k_{\parallel} - k_{\perp}$  is obviously zero and shows a clear discontinuity at the N-I transition. Such discontinuity is related to the first-order nature of this transition. It should be noted that although the photopyroelectric technique is an ac calorimetric technique, it can be used for a straightforward determination of the order of a phase transition, thanks to its sensitivity to anisotropy in the heat diffusion process. This aspect, combined with the ability of the technique to measure simultaneously and with a high resolution the critical behavior of static quantities, such as the specific heat, and dynamic quantities, such as the thermal conductivity, makes it unique for the study of thermal parameters close to phase transitions. It should be noted that other high-resolution ac calorimetric techniques [18] have been used previously to assess the order of a phase transition. In particular the behavior of the phase lag of the measured ac signal was related to the presence of a latent heat, but this was only possible in a quite indirect and qualitative way.

The anisotropy of  $k$  in 9CB increases with decreasing temperature in the nematic and smectic phases and resembles the behavior of  $k_{\parallel}$ . This can be easily explained considering the much weaker temperature dependence of  $k_{\perp}$  with respect to  $k_{\parallel}$ . Just below  $T_{AN}$  there is a rapid increase of the anisotropy with decreasing temperature. Approximately one degree below  $T_{AN}$ , the rate of change of the anisotropy decreases and  $k_{\parallel} - k_{\perp}$  tends to approach a saturation value.

The temperature dependence of  $k_{\parallel} - k_{\perp}$  of 8CB has been obtained from the data reported in Ref. [5]. The behavior is approximately the same as the one reported for 9CB. A discontinuity at the N-I transition and a continuous behavior at the A-N one, which has been confirmed by high-resolution temperature scans (not shown), have been found. The increase of the anisotropy below  $T_{AN}$  seems to be less pronounced in this case than in 9CB. To check whether this effect is related to the width of the nematic range, we have

also shown the anisotropy measurements on  $\overline{8S5}$ . The anisotropy shows a smooth behavior over  $T_{AN}$ , where it seems to have reached the saturation value.

Figure 9 shows high-resolution measurements of  $k_{\parallel} - k_{\perp}$  close to the  $A-N$  transition. No discontinuity can be detected in the transition region and this leads to the conclusion that, within the resolution of our technique, the  $A-N$  transition in 9CB is of second order. It could be, however, that the resolution of our technique is not high enough to detect discontinuity in the order parameter in very weakly first-order phase transitions. As already stated, the resolution can be estimated from the rounding region that in the case of our measurements on 8CB was about 5 mK from  $T_{AN}$  on either side of the transition. This resolution, in the case of specific-heat measurements, is comparable with the resolution of other ac calorimetric techniques [18], but lower than the one of adiabatic scanning calorimetry (ASC), which is at least 0.001 K [19]. The results we have obtained from the fit of  $c$  data are, however, in good agreement with the ones obtained with ASC. ASC measurements in 8CB at the  $A-N$  transition give an upper limit for the latent heat of 0.4 J/mol and Thoen, Marynissen, and van Dael concluded that the transition is a second-order one [19], but recent measurements on the movement of interfaces between the nematic and smectic phases [20,21] seem to suggest a very weak first-order nature. It is important to point out, however, that the main characteristic of the photopyroelectric technique is its ability to perform high-resolution measurements for the study of the critical behavior of dynamic as well as static thermal properties.

## DISCUSSION

The behavior of the thermal conductivity in all the samples investigated can be tentatively explained using the simple arguments introduced by Rondelez, Urbach, and Hervet [8], which suggest an analogy between the elongated liquid crystal molecules and grains in a polycrystalline solid. The thermal conductivity in these materials is limited by the grain size since the phonon mean free path cannot exceed this dimension. Now, considering the molecules as rigid rods and assuming that the intramolecular thermal conductivity is exceedingly high with respect to the intermolecular one, it turns out that the heat diffusion in a given direction is dominated by the number of interfaces among molecules encountered in that direction. The number of interfaces for a fixed sample thickness is larger for a planar sample than for a homeotropic one and therefore the thermal conductivity should be larger in the latter case. This is what has been observed in many liquid-crystal compounds [5,8,22–25]. Following this approach, the thermal conductivity temperature dependence should be somehow related to the temperature dependence of the molecules alignment and therefore of the microscopic orientational order parameter  $S$ . The increase of  $S$  with decreasing temperature should correspond to an increase of  $k_{\parallel}$  and a decrease of  $k_{\perp}$ . The results obtained for  $k_{\parallel}$  in this work, as well as the ones found in literature, confirm this hypothesis [5,22–25]. The situation is more complicated in the case of  $k_{\perp}$ , which shows a weaker temperature dependence with respect to  $k_{\parallel}$ , a result that is difficult to explain in terms of the simple description pro-

posed by Rondelez, Urbach, and Hervet. In 9CB,  $k_{\perp}$  decreases (slightly) in the nematic phase as a function of temperature, but remains fairly constant in the smectic one. A similar behavior has been found in 8CB [5] and in  $\overline{8S5}$ , where the decrease of  $k_{\perp}$  with temperature in the nematic phase is more evident because of the progressive increase of the nematic range. In both cases the  $k_{\perp}$  temperature dependence is weaker than the  $k_{\parallel}$  one. Similar results for  $k_{\perp}$  have been found also for 4,4'-di-hexylazoxybenzene (6AB) [22] and 4-*n*-pentyl-4'-cyanobiphenyl (5CB) [23] below  $T_{NI}$ . To explain the above mentioned behavior of  $k_{\parallel}$  and  $k_{\perp}$ , one should assume that  $k$  is more sensitive to variations of the molecular long axis direction around the average alignment one in the homeotropic case than in the planar one. Another possible explanation could be the that the degree of alignment which can be achieved in the case of planar samples with the various procedures is always poorer than the one obtained in the homeotropic one. In fact, the above mentioned behavior of  $k_{\perp}$  was observed using different procedures for the alignment such as rubbing (6AB) [22], magnetic field (5CB) [23] and quartz deposition (this work). An even more complicated temperature dependence for  $k_{\perp}$  has been found in *N*-(4-methoxybenzylidene)-4'-butylaniline (MBBA) [24], *p*-azoxyanisole (PAA), and *p*-butoxybenzylidene-*p*-*n*-octylaniline (BBOA) [25], where after a minimum below  $T_{NI}$ , it was found to increase with decreasing temperature. This behavior is surprising since it could lead, as in the case of Ref. [24], to an order parameter that, after a peak below  $T_{NI}$ , unrealistically decreases with temperature.

All these considerations clearly show not only the success but also the limits of the simple description proposed by Rondelez, Urbach, and Hervet [8] and lead to the conclusion that more effort is needed to clarify the mechanisms of thermal conduction in liquid crystals. In this respect measurements on the *n*CB homologous series, with a goal of clarifying the role of the molecular shape and interactions, are presently being taken and will be presented elsewhere.

The proposed mechanism for the heat conduction in liquid crystals basically assumes that the thermal conductivity is dominated by short-range processes. What happens when the transition temperature is approached? Collective phenomena due to the divergence of the correlation length and therefore long-range interactions take place and these interactions are responsible for the anomaly observed in many physical quantities. In dynamics, long-range interactions lead to possible coupling of long-lived modes. If the coupling is non-dissipative, a divergence in the thermal conductivity is expected, while if it is dissipative, it remains finite [7]. It could be, however, that short-range processes dominate close to the transition temperature, which could also give a smooth conductivity all over the transition region. The results reported in Fig. 5 show no anomaly in the thermal conductivity of 9CB at the  $A-N$  phase transition as in the case of 8CB and  $\overline{8S5}$ , thereby ruling out the possibility of a nondissipative coupling between the order parameter mode and the energy density.

9CB is known to be very close to the  $A-N$  tricritical point. Nonetheless, the behavior of the thermal conductivity close to the transition temperature is similar to the ones observed in 8CB and  $\overline{8S5}$ , which have an increasingly wider nematic range. These results suggest that for the  $A-N$  transition there

is no influence of tricriticality on the behavior of  $k$ . On the contrary, as already stated, it has been suggested that in the case of the  $A$ - $C$  transition [4] tricriticality substantially affects the critical behavior of  $k$ , which in all the reported cases showed a divergence [3,4].

The proximity of the  $A$ - $N$  and  $N$ - $I$  transitions, however, seems to have an effect on  $k_{\parallel}$ - $k_{\perp}$  close to  $T_{AN}$  since the change in slope of this quantity just below the transition temperature is much more pronounced in 9CB than in 8CB and is practically absent in 8S5. Considering the coupling between the smectic and the nematic order parameters, it turns out that smectic layering induces an increase in the orientational order parameter given by  $\delta S = S - S_0(T) = \chi C \rho_1^2$  [17], where  $S_0(T)$  is the order parameter in the absence of the smectic phase,  $C$  is a constant,  $\rho_1$  is the first harmonic of the density modulation in the smectic phase, and  $\chi(T)$  is a response function that increases upon approaching  $T_{NI}$ . The observed behavior of  $k_{\parallel}$ - $k_{\perp}$  is therefore related to a decreasing coupling of  $S$  and  $\rho_1$  going from 9CB to 8CB and 8S5 because of the increase in the nematic range. In other words, as  $T_{AN}$  progressively moves away from  $T_{NI}$ ,  $S_0$  tends to saturate and cannot substantially change any longer when the smectic ordering also occurs. A similar contribution of smectic ordering to the nematic order parameter has been reported in a mixture of 8CB and 10CB in the isotropic phase close to  $T_{NI}$  as a function of applied field and  $\delta S$  has been estimated [26]. Finally, it should be noted that from a more accurate analysis of the previously reported data of the

thermal conductivity at  $T_{AN}$  in 8CB [5], it turns out that what had been described as a minor increase in  $k$  around  $T_{AN}$  was in reality a change in slope similar to the ones described above.

## CONCLUSIONS

Measurements of the specific heat, thermal conductivity, and thermal diffusivity have been performed on three compounds with MacMillan ratios of 0.936 and 0.977 and 0.994, respectively. It has been found that in all the cases  $k$  remains approximately constant close to  $T_{AN}$  and the thermal conductivity critical behavior at the  $A$ - $N$  transition is not affected by tricriticality. Results on the temperature dependence of  $k_{\parallel}$  and  $k_{\perp}$  for all the compounds investigated have been reported and they have been discussed according to a description given by Rondelez, Urbach, and Hervet, which assumes that the thermal conductivity is strongly affected by the shape of the liquid-crystal molecule. It has been possible with the photopyroelectric technique to study the behavior of the macroscopic orientational order parameter  $k_{\parallel}$ - $k_{\perp}$  as a function of temperature and thus determine the order of the phase transition. It turns out that also in the case of 9CB, within the limit of our experimental resolution, the  $A$ - $N$  transition is a second-order one. The influence of smectic layering on the order orientational parameter has been reported and it has been shown that it becomes less important when the nematic range increases.

- 
- [1] M. Marinelli, F. Mercuri, U. Zammit, and F. Scudieri, *Phys. Rev. E* **53**, 701 (1996).
- [2] G. Nounesis, C. C. Huang, and J. W. Goodby, *Phys. Rev. Lett.* **56**, 1712 (1986).
- [3] E. K. Hobbie and C. C. Huang, *Phys. Rev. A* **36**, 5459 (1987).
- [4] E. K. Hobbie, H. Y. Liu, C. C. Huang, Ch. Bahr, and G. Heppke, *Phys. Rev. Lett.* **67**, 1771 (1991).
- [5] M. Marinelli, F. Mercuri, S. Foglietta, U. Zammit, and F. Scudieri, *Phys. Rev. E* **54**, 1604 (1996).
- [6] M. Marinelli, F. Mercuri, S. Foglietta, and D. P. Belanger, *Phys. Rev. B* **54**, 4087 (1996).
- [7] P. C. Hohenberg and B. I. Halperin, *Rev. Mod. Phys.* **49**, 435 (1977).
- [8] F. Rondelez, W. Urbach, and H. Hervet, *Phys. Rev. Lett.* **41**, 1058 (1978).
- [9] M. Marinelli, F. Mercuri, U. Zammit, R. Pizzoferrato, F. Scudieri, and D. Dadarlat, *Phys. Rev. B* **49**, 9523 (1994).
- [10] D. A. Dunmur and W. H. Miller, *J. Phys. Colloq.* **40**, C3-141 (1979).
- [11] H. Marynissen, J. Thoen, and W. Van Dael, *Mol. Cryst. Liq. Cryst.* **97**, 149 (1983).
- [12] A. Aharony and G. Ahlers, *Phys. Rev. Lett.* **44**, 782 (1980).
- [13] M. E. Fisher and S. Sarbach, *Phys. Rev. Lett.* **41**, 1127 (1978); S. Sarbach and M. E. Fisher, *Phys. Rev. B* **20**, 2797 (1979).
- [14] H. Marynissen, J. Thoen, and W. Van Dael, *Mol. Cryst. Liq. Cryst.* **124**, 195 (1985).
- [15] U. Zammit, M. Marinelli, R. Pizzoferrato, F. Scudieri, and S. Martellucci, *Phys. Rev. A* **41**, 1153 (1990).
- [16] M. Marinelli, U. Zammit, R. Pizzoferrato, F. Scudieri, S. Martellucci, and F. Mercuri, in *Phase Transition in Liquid Crystals*, edited by S. Martellucci and A. N. Chester (Plenum, New York, 1992), p. 227.
- [17] P. G. de Gennes and J. Prost, *The Physics of Liquid Crystal* (Clarendon, Oxford, 1993).
- [18] CW. Garland, in *Liquid Crystals: Physical Properties and Phase Transitions*, edited by S. Kumar (Cambridge University, Cambridge, in press), Chap. 6.
- [19] J. Thoen, H. Marynissen, and W. van Dael, *Phys. Rev. A* **26**, 2886 (1982).
- [20] P. E. Cladis, W. van Saarloos, D. A. Huse, J. S. Patel, J. W. Goodby, and P. L. Finn, *Phys. Rev. Lett.* **62**, 1764 (1989).
- [21] N. Tamblyn, P. Oswald, A. Miele, and J. Bechhoefer, *Phys. Rev. E* **51**, 2223 (1995).
- [22] J. Caerels, E. Schoubs, and J. Thoen, *Liq. Cryst.* (to be published).
- [23] G. Ahlers, D. S. Cannel, L. I. Berge, and S. Sakurai, *Phys. Rev. E* **49**, 545 (1994).
- [24] R. Vilanove, E. Guyon, C. Mitescu, and P. Pieranski, *J. Phys. (France)* **35**, 153 (1974).
- [25] W. Urbach, H. Hervet, and F. Rondelez, *Mol. Cryst. Liq. Cryst.* **46**, 209 (1978).
- [26] I. Lelidis and G. Durand, *Phys. Rev. Lett.* **73**, 672 (1994).